

A topologically flat thick 2-brane on higher dimensional black hole backgrounds

Viktor G. Czinner^{1,2,*}

¹*Department of Mathematics and Applied Mathematics, University of Cape Town, Rondebosch, 7701, South Africa;*

²*Department of Theoretical Physics, MTA KFKI Research Institute for Particle and Nuclear Physics, Budapest 114, P.O. Box 49, H-1525, Hungary*

We present a numerical solution for a topologically flat 2-dimensional thick brane on a higher dimensional, spherically symmetric black hole background. Present solution is the last, missing part of the complete set of solutions for the thickness corrected brane - black hole problem in arbitrary number of dimensions. We show that the 2-dimensional case is special compared to all the higher dimensional solutions in the topologically Minkowskian family as being non-analytic at the axis of the system. We provide the numerical solution in the near horizon region and make a comparison with the infinitely thin case.

PACS numbers: 04.70.Bw, 04.50.-h, 11.27.+d

I. INTRODUCTION

The study of higher dimensional black holes, branes and their interactions is an active field of research in several different areas of modern theoretical physics [1–4]. One interesting direction, which has been first introduced by Frolov [2], is to consider a brane - black hole (BBH) toy model for studying merger and topology changing transitions in higher dimensional classical general relativity [5, 6], or in certain strongly coupled gauge theories [3, 7] through the AdS/CFT correspondence [8]. Generalizations of the BBH model by studying thickness corrections to the Dirac-Nambu-Goto effective brane action [9–11] from higher order curvature terms, have also been studied recently, first by perturbative approaches [12, 13], and later within an exact description [14].

The results of the perturbative approaches concluded that there is a "symmetry breaking" between the two topologically different solution family, as regular perturbative solutions do not exist for Minkowskian embedding topologies except in the special case of a 2-brane. The problem, on the other hand, can be solved regularly for any brane dimensions in the black hole embeddings. This virtual "symmetry breaking" phenomenon obtained a simple resolution in [13], where it was pointed out that perturbative thick solutions break down around their thin counterparts for Minkowski topologies, because the thin solutions are not analytic at the axis of the system. Motivated by this observation, in [14], a general family of thick solutions could be provided for both topologies within a non-perturbative numerical approach for all but one exceptional case. The exception, mysteriously, turned out to be the same case, where the regular perturbative solution existed, namely the 2-dimensional, topologically flat case.

The above findings of [14] naturally raised the question: How can a regular perturbative solution exist in

the same single case where the regular non-perturbative solution can not be found?

In the present paper we provide the answer to this question and obtain the so far missing solution of the topologically flat 2-brane in arbitrary number of bulk dimensions for the thick-BBH system. By including this solution, we complete the full set of solutions of the problem that we started presenting first with a perturbative approach in [13] and continued with a non-perturbative description in [14]. The present work, therefore, is the final part of the series of papers we addressed to the thickness corrected BBH problem and we kindly refer the reader also to [13, 14] for the more detailed model setups and for all those definitions, notations and results that might be missing here and would make the present paper completely self-contained.

The plan of the paper is as follows. In Sec. II, we provide a short overview on the thin- and thick-BBH model setups. In Sec. III we obtain the special case of the 2-brane equation, and in Sec. IV we analyze its regularity conditions for flat topology. In Sec. V we provide the non-perturbative, numerical solution of the problem in the near horizon region, and in Sec. VI we draw our conclusions.

II. THE BRANE - BLACK HOLE SYSTEM

Let us overview quickly the most important properties of the thin-BBH system introduced by Frolov in [2], and its thickness corrected generalization provided in [13].

A. The thin model

We consider static brane configurations in the background of a static, spherically symmetric bulk black hole. The metric of an N -dimensional, spherically symmetric black hole spacetime is

$$ds^2 = g_{ab}dx^a dx^b = -f dt^2 + f^{-1} dr^2 + r^2 d\Omega_{N-2}^2, \quad (1)$$

* czinner@rmki.kfki.hu

where $f = f(r)$ and $d\Omega_{N-2}^2$ is the metric of an $N - 2$ dimensional unit sphere. One can define coordinates $\theta_i (i = 1, \dots, N - 2)$ on this sphere with the relation

$$d\Omega_{i+1}^2 = d\theta_{i+1}^2 + \sin^2 \theta_{i+1} d\Omega_i^2 . \quad (2)$$

The explicit form of f is not important, it is only assumed that f is zero at the horizon r_0 , and it grows monotonically to 1 at the spatial infinity $r \rightarrow \infty$, where it has the asymptotic form [15],

$$f = 1 - \frac{r_0}{r^{N-3}} . \quad (3)$$

In the zero thickness case the test brane configurations in an external gravitational field can be obtained by solving the equation of motion coming from the Dirac-Nambu-Goto action [9–11],

$$S = \int d^D \zeta \sqrt{-\det \gamma_{\mu\nu}} , \quad (4)$$

where $\gamma_{\mu\nu}$ is the induced metric on the brane

$$\gamma_{\mu\nu} = g_{ab} \frac{\partial x^a}{\partial \zeta^\mu} \frac{\partial x^b}{\partial \zeta^\nu} , \quad (5)$$

and $\zeta^\mu (\mu = 0, \dots, D - 1)$ are coordinates on the brane world sheet. The brane tension does not enter into the brane equations, thus for simplicity it can be put equal to 1. It is also assumed that the brane is static and spherically symmetric, and its surface is chosen to obey the equations

$$\theta_D = \dots = \theta_{N-2} = \pi/2 . \quad (6)$$

With the above symmetry properties the brane world sheet can be defined by the function $\theta_{D-1} = \theta(r)$ and we shall use coordinates ζ^μ on the brane as

$$\zeta^\mu = \{t, r, \phi_1, \dots, \phi_n\} \quad \text{with} \quad n = D - 2 . \quad (7)$$

The parameter n denotes the number of dimensions in which the brane is rotationally symmetric. In this paper we consider the special case of $n = 1$, i.e. a 3-dimensional brane world sheet, that is a 2-dimensional, axisymmetric brane embedded into the higher dimensional black hole spacetime.

With this parametrization the induced metric on the brane is

$$\gamma_{\mu\nu} d\zeta^\mu d\zeta^\nu = -f dt^2 + \left[\frac{1}{f} + r^2 \dot{\theta}^2 \right] dr^2 + r^2 \sin^2 \theta d\Omega_n^2 , \quad (8)$$

where, and throughout this paper, a dot denotes the derivative with respect to r , and the action (4) reduces to

$$S = \Delta t \mathcal{A}_n \int \mathcal{L}_0 dr , \quad (9)$$

$$\mathcal{L}_0 = r^n \sin^n \theta \sqrt{1 + fr^2 \dot{\theta}^2} , \quad (10)$$

where Δt is the interval of time and $\mathcal{A}_n = 2\pi^{n/2}/\Gamma(n/2)$ is the surface area of a unit n -dimensional sphere.

B. Thickness corrections

In the case of a thick brane, the curvature corrected effective brane action is obtained by Carter and Gregory in [16], and the corrections to the thin DNG action are induced by small thickness perturbations as

$$S = \int d^D \zeta \sqrt{-\det \gamma_{\mu\nu}} \left[-\frac{8\mu^2}{3\ell} (1 + C_1 R + C_2 K^2) \right] , \quad (11)$$

where R is the Ricci scalar, K is the extrinsic curvature scalar of the brane and the coefficients C_1 and C_2 are expressed by the wall thickness parameter ℓ as

$$C_1 = \frac{\pi^2 - 6}{24} \ell^2 , \quad C_2 = -\frac{1}{3} \ell^2 . \quad (12)$$

The parameter μ is related to the thickness by

$$\ell = \frac{1}{\mu \sqrt{2\lambda}} \quad (13)$$

which originates from a field theoretical domain-wall model where μ is the mass parameter and λ is the coupling constant of the scalar field.

After integrating out the spherical symmetric part and the time dependence on the introduced static, spherically symmetric, higher dimensional black hole background, one obtains (see also [13])

$$S = \Delta t \mathcal{A}_n \int \mathcal{L} dr , \quad (14)$$

$$\mathcal{L} = -\frac{8\mu^2}{3\ell} \mathcal{L}_0 [1 + \varepsilon \delta] , \quad (15)$$

where we introduced the notations

$$\varepsilon = \frac{\ell^2}{L^2} , \quad \delta = aK^2 + bQ , \quad (16)$$

with

$$Q = K_b^a K_a^b , \quad a = \frac{\pi^2 - 14}{24} L^2 , \quad b = \frac{6 - \pi^2}{24} L^2 . \quad (17)$$

Here L is the relevant dynamical length scale of the system which has to be large compared to the thickness parameter ℓ in order to (11) remain valid. The explicit expressions of the curvature scalars K and Q are given in (35) and (36) of [13].

For a detailed introduction of both the thin- and thick-BBH systems, please refer to [2, 13].

III. THE 2-BRANE EQUATION

From this section on we will focus only on the case of the topologically flat or Minkowskian 2-brane. In two dimensions "topologically flat" is synonymous with "topologically Minkowskian", and we retain both terms for the sake of elegant variation.

In order to obtain the 2-brane equation of motion, first we observe that the thickness corrected DNG-brane action is a function of the second derivative of θ and thus the Euler-Lagrange equation of the problem has the form (see for example [17])

$$\frac{d^2}{dr^2} \left(\frac{\partial \mathcal{L}}{\partial \ddot{\theta}} \right) - \frac{d}{dr} \left(\frac{\partial \mathcal{L}}{\partial \dot{\theta}} \right) + \frac{\partial \mathcal{L}}{\partial \theta} = 0. \quad (18)$$

From (18) the actual equation of motion becomes

$$\theta^{(4)} + T_1 \theta^{(3)} + T_2 (\ddot{\theta}, \dot{\theta}, \theta, f^{(3)}, \ddot{f}, \dot{f}, f, r) = 0, \quad (19)$$

where, in the 2-dimensional ($n = 1$) case

$$T_1 = \frac{1}{rfF^2} [6f + 4rf + 2rf \cot \theta \dot{\theta} - r^2 f (4f + rf) \dot{\theta}^2 + 2r^3 f^2 \cot \theta \dot{\theta}^3 - 10r^3 f^2 \dot{\theta} \ddot{\theta}], \quad (20)$$

with

$$F = \sqrt{1 + fr^2 \dot{\theta}}, \quad (21)$$

and T_2 is given in the Appendix.

As it is immediate to see, (19) is a 4th-order, highly nonlinear equation, and it is probably impossible to present its solutions in closed, analytic form. Hence, the goal of this paper, is to provide a regular, numerical solution of (19) in arbitrary bulk dimensions for flat topology.

IV. REGULARITY AND BOUNDARY CONDITIONS

It was pointed out first in [13], that the brane solutions obtained by Frolov in [2] are regular but not analytic (or smooth) at the axis of the thin-BBH system for the Minkowski embedding branch. In fact they are not even differentiable at that point and thus belong to the class of C^0 functions only. According to this property, and since we found that the perturbative approach broke down around these solutions for the thick case, we concluded that the thick brane solutions must behave significantly differently at the axis of the system, namely we expected them to be smooth there. It was surprising however that in the single case of the 2-brane, a regular perturbative solution existed. We gave a detailed analysis of this solution in [13].

In [14], approaching the problem by a new, non-perturbative numerical method, we looked for the missing solutions of the Minkowski branch in the class of analytic functions. We obtained regular boundary conditions at the axis of the system by considering the series expansion of the exact 4th-order equation of motion around $\theta = 0$. With this method we successfully provided all the missing, topologically Minkowskian solutions of the thick-BBH system, except in the curious case of the 2-brane again.

It was obvious, of course, that a perturbative solution can not exist without the existence of a non-perturbative

solution, and also since explicitly constructed, field theoretical domain wall solutions [18, 19] clearly exist in the case of the 2-brane, we suspected that the lack of this solution must lie somewhere in the validity of the applied method. Nevertheless, we were so enthusiastic with providing the whole family of the missing solutions in the C^∞ class at the axis, that it didn't occur in our mind at the time, that the 2-dimensional case might be special in the topologically Minkowskian family as being the only one which is non-analytic at the axis.

The main result of the present paper is the observation, that the 2-dimensional solution of the thick-BBH system is in fact a special one in the topologically Minkowskian family as being C^0 (or as we will soon see maximum C^1) function at the axis of the system. All the other dimensional solutions are C^∞ . This also explains the fact why it was only the 2-dimensional case where a perturbative solution could exist around the thin solution.

In the remaining of this section we analyze the asymptotic behavior of (19) near the axis of the system. We obtain necessary boundary conditions from regularity requirements and show that these conditions can always be fulfilled in order to obtain a regular solution.

Asymptotic analysis

We know from the above considerations that a regular solution of the problem must exist although analytic solution could not be found at the axis of the system. Thus the point r_1 on the axis, where $\theta(r_1) = 0$, must be a *regular singular point* of the differential equation (19). Even though (19) is highly nonlinear, general results from the theory of *local* analysis of linear differential equations can be applied, because we know from physical considerations that (19) should not develop any nontrivial singular points in its domain.

Hence, if a solution is not analytic at a regular singular point (see e.g. [20]), its singularity must be either a pole or an algebraic or logarithmic branch point, and there is always at least one solution of the form

$$\theta(r) = (r - r_1)^\alpha A(r) \quad (22)$$

where α is a number called *indicial exponent* and $A(r)$ is a function which is analytic at r_1 and has a convergent Taylor series.

In the general case α can be any number that solves (19). In our specific case however, the thin solution, around which a regular perturbative solution existed, had the asymptotic form near r_1 (see [2, 13])

$$\theta(r) = \eta \sqrt{r - r_1} + \dots, \quad (23)$$

and similarly, the corresponding perturbative solution (see [13]) near the same point had the asymptotic form

$$\theta_{thick} \equiv \theta_{thin} + \varepsilon \varphi = (\eta + \varepsilon \kappa) \sqrt{r - r_1} + \dots, \quad (24)$$

where φ is the perturbation function and η and κ are coefficient functions defined in [13]. Thus, in order to obtain the non-perturbative thick solution, we also chose α to be $1/2$, in accordance with the perturbative results. This choice will also have the advantage of naturally fixing the free boundary condition in the next section for a unique numerical solution.

With $\alpha = 1/2$, from (22) we obtain that the asymptotic form of $\theta(r)$ near the axis is

$$\begin{aligned} \theta(r) = & A_1\sqrt{r-r_1} + A_2(r-r_1)^{\frac{3}{2}} \\ & + A_3(r-r_1)^{\frac{5}{2}} + A_4(r-r_1)^{\frac{7}{2}} + \dots \end{aligned} \quad (25)$$

Plugging this expression and its derivatives into (19), one can obtain the following asymptotic behavior

$$\frac{c_5}{(r-r_1)^{\frac{5}{2}}} + \frac{c_3}{(r-r_1)^{\frac{3}{2}}} + \frac{c_1}{\sqrt{r-r_1}} + c_0 + \dots = 0, \quad (26)$$

where the coefficient functions c_i are polynomial expressions of A_i with dependences

$$\begin{aligned} c_5 &= c_5(A_1, A_2) \\ c_3 &= c_3(A_1, A_2, A_3) \\ c_1 &= c_1(A_1, A_2, A_3, A_4). \end{aligned}$$

In order to obtain a regular solution, we need to require for the c_i coefficient functions to disappear at r_1 . From the explicit forms of c_i , one can find that the coefficient A_1 can be chosen freely, and once it's fixed, the remaining coefficients A_2 , A_3 and A_4 can be computed from the requirements that $c_i(r_1) = 0$. Consequently, the solution is uniquely determined by the parameter r_1 (i.e. the minimal distance parameter), and the explicit values of the coefficients A_2 , A_3 and A_4 can be immediately obtained from the $c_i(r_1) = 0$ equations. (This procedure is of course necessary before the numerical setup.) For the question of existence, the $c_i(r_1) = 0$ equations are always soluble, as it turns out that these are linear equations for the A_i coefficients. The explicit forms of the coefficients A_2 , A_3 and A_4 , as successive functions of A_1 and r_1 are given in the Appendix.

In conclusion we found that a regular 2-dimensional solution can always be given for the exact problem, and a unique solution is completely determined by the regularity requirements once the coefficient A_1 is fixed. Since we are free to choose A_1 , it can also put to be 0 for example. In this case the asymptotic form (25) starts with

$$\theta(r) = A_2(r-r_1)^{\frac{3}{2}} + \dots, \quad (27)$$

which solution is a C^1 function, however in all other cases the solution of (19) is C^0 at r_1 .

V. NUMERICAL SOLUTION NEAR THE HORIZON

For illustrating the obtained results, we provide the numerical solution of the 2-dimensional flat problem. With

the experiences we gained from the analysis of the thick-BBH system in [13, 14], it is not too difficult to obtain the numerical solution here, after the initial conditions for this specific case has been clarified.

As we discussed earlier, we are free to choose the coefficient A_1 in the asymptotic solution (25). Nevertheless, in order to be completely consistent with our previous perturbative results in the flat 2-brane case, we make the choice

$$A_1 = \eta + \varepsilon\kappa \quad (28)$$

that was forced upon us by regularity requirements for the perturbations. Having fixed this freedom, the remaining three conditions A_2 , A_3 and A_4 are determined, as discussed in the previous section, and the corresponding numerical solution is unique.

In obtaining the numerical solution we used Mathematica[®] `NDSolve` function. The integration range went from r_1 until 1000 to check the accordance with the corresponding perturbative solution.

The configurations of the perturbative thick 2-brane solutions in the near horizon region have been presented in [13]. Since the effects of the nonlinearities are really small even in the gravitationally strong, near horizon region, the overall global picture of the thickness corrected brane configurations remain very similar to the perturbative case. To make however the small effects visible, we plot on Fig. 1 and Fig. 2 the difference function

$$\Delta\theta(r) = \theta(r) - \theta_{DNG}(r),$$

of the present thick- and the original thin solutions in 4 and 5 dimensions. $\Delta\theta(r)$ is the exact analog of the perturbation function $\varepsilon\varphi(r)$ defined in (24).

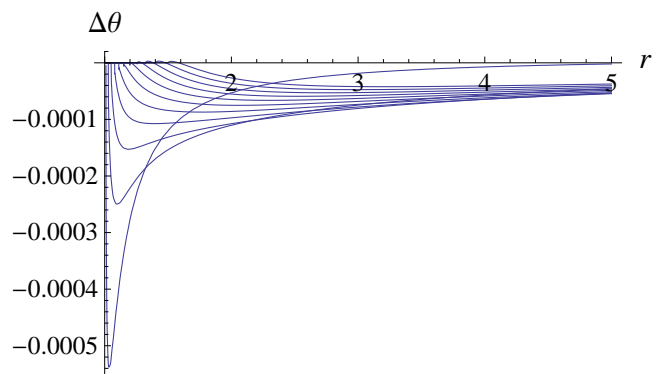


FIG. 1. The picture shows a sequence of near horizon $\Delta\theta(r)$ curves in 4 dimensions with minimum horizon distance range $1.01 \leq r_1 \leq 2$.

Comparing the results with the corresponding plots of the perturbative solutions in [13], we find that the general behavior of the $\Delta\theta(r)$ curves are essentially the same. This is of course what one expects. On the other hand one also expects some differences coming from the nonlinear regime of (19), and those are also present if

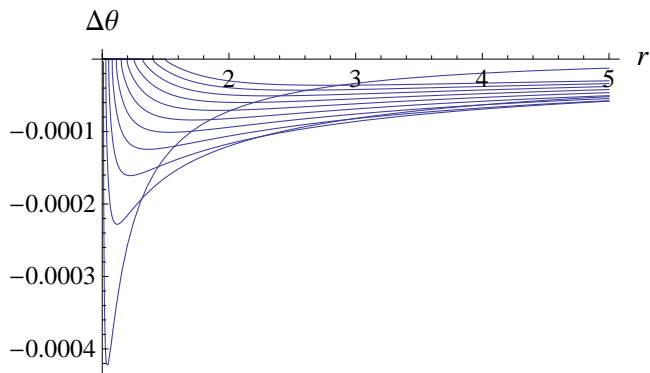


FIG. 2. The same sequence of $\Delta\theta(r)$ curves as on FIG.1 in 5 dimensions.

we enlarge the very near horizon region of the individual curves. The main features of these differences are plotted on Fig. 3 and Fig. 4.

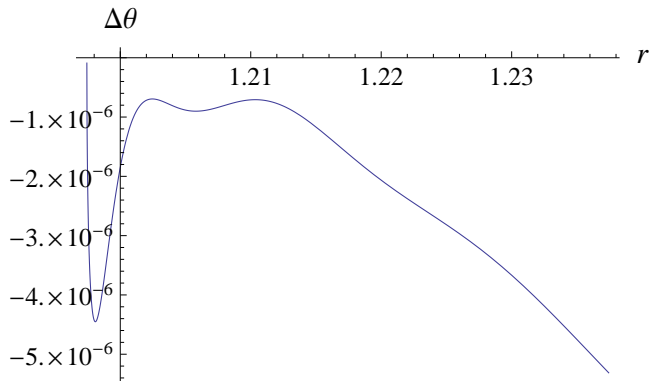


FIG. 3. Near horizon nonlinear effects on a $\Delta\theta(r)$ curve in 4 dimensions with minimum horizon distance $r_1 = 1.19744$.

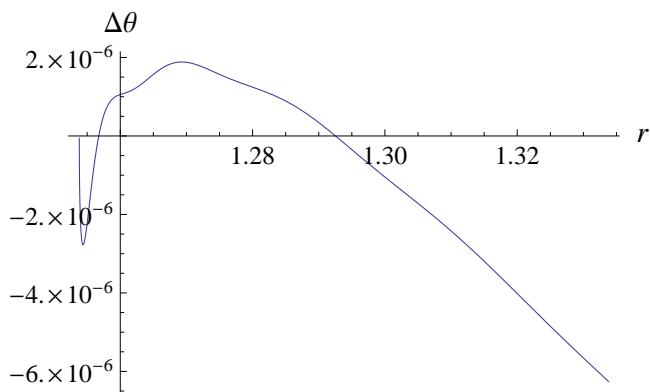


FIG. 4. Near horizon nonlinear effects on a $\Delta\theta(r)$ curve in 4 dimensions with minimum horizon distance $r_1 = 1.2538$.

On Fig. 3 an interesting nonlinear effect appears compared to the perturbative solution. Instead of monotonically decreasing down to its global minimum, as φ does

in the perturbative case, the $\Delta\theta(r)$ curve has an extra local pattern near the minimum horizon distance r_1 . The extra pattern is that the curve goes through some additional local extrema in this region before it finally tends to reach the global minimum which is similar to the one in the perturbative case. During these local differences however, $\Delta\theta(r)$ remains negative in this whole region.

On the qualitatively similar curve on Fig. 4, the essential difference compared to Fig. 3 is that $\Delta\theta(r)$ develops a sign change in this region, that is there are several intersections in the very near horizon region between the thick and thin solutions compared to the single intersection that is present in the case of the perturbative solution (see Fig. 6 in [13]).

With increasing horizon distance r , the above nonlinearities decay quickly, and the solution agrees very well with the perturbative results.

VI. CONCLUSIONS

In the present work we studied the problem of a topologically flat 2-brane in a higher dimensional, thickness corrected BBH system. We provided a regular, non-perturbative, numerical solution for this special case based on earlier perturbative considerations [13]. The main result of this paper is the observation that the 2-dimensional case of the problem is a special one as being non-analytic at the axis of the system. This property makes it unique in the family of thick solutions, as in all other dimensions both the Minkowski and black hole embedding solutions are analytic in their entire domain.

We analyzed the asymptotic behavior of the solution and obtained that it is at most a C^1 , but in the general case it is only a C^0 function at the axis, just like the corresponding thin solutions. The initial conditions of the problem are not uniquely fixed by regularity requirements, thus the solution we provided here is not unique. It is however perfectly consistent with our earlier perturbative results.

With the present paper, we have provided the complete set of solutions of the thick-BBH problem in a series of three consecutive papers. First, in [13], we obtained all possible perturbative solutions and later, in [14] all non-perturbative solutions were given except the case of the flat 2-brane. Present work completes the set.

In [13] we analyzed the properties of a topology changing, quasi-static phase transition in the thick-BBH system. The obtained results in the present case however does not change our previous findings and thus we don't consider the phase transition in this paper.

The result, that thickness corrections change the analytic properties of the brane solutions at the axis of the system might have some physical consequences. Infinitely thin brane solutions, naturally, are very important in higher dimensional physics, but considering the present problem, one has the intuition that the thickness corrections, which are in agreement with field theoretic

domain wall models, made the thin-BBH system more stable in the sense that regular, analytic solutions could be provided in essentially all cases. Since small physical perturbations to any system are usually proportional to the derivatives of the unperturbed solution, it is very possible that the thin-BBH solutions are not entirely stable against small perturbations in the Minkowski branch. (Stability properties of the BBH system for the analytic black hole embedding solutions has been studied for example in [21].) This property however has been cured by the thickness corrections and it is somehow in accordance with our physical expectations.

The special case of the 2-brane as “remaining“ non-analytic after thickness corrections, thus, is an unexpected property, which makes it physically interesting. So much the more that thick 2-branes, i.e. thin walls on

black hole backgrounds in standard 4-dimensional general relativity are certainly real, physical objects. The fact that these solutions are essentially different from the corresponding ones in higher dimensions is remarkable.

ACKNOWLEDGMENTS

Most part of the calculations were performed and checked using the computer algebra program MATHEMATICA 7. The research was supported by the National Research Foundation of South Africa and the Hungarian National Research Fund, OTKA No. K67790 grant.

Appendix: Coefficient Functions

$$\begin{aligned}
T_2 = & \frac{1}{64(a+b)\varepsilon f^2 r^4 F^4} [(\varepsilon f^3 r^6 \dot{\theta}^3 (-8(10a+7b) + 18(2a+3b)fr^2\dot{\theta}^2 \\
& + 6(2a+b)f^2r^4\dot{\theta}^4 + (a+b)f^3r^6\dot{\theta}^6) - 2\varepsilon f^2r^3(-12(10a+7b)\dot{\theta} + 2(126a+109b)fr^2\dot{\theta}^3 \\
& + 90af^2r^4\dot{\theta}^5 + 3(13a+5b)f^3r^6\dot{\theta}^7 + 2(3a+b)f^4r^8\dot{\theta}^9 - 4(18a+17b)r\ddot{\theta} + (5a+b)f^3r^7\dot{\theta}^8 \cot \theta \\
& + 2r\dot{\theta}^2(3(46a+43b)fr^2\ddot{\theta} + (-26a-7b)\cot \theta) - f^2r^5\dot{\theta}^6 \csc \theta(-23(a+b)\cos \theta + (5a+b)fr^2\ddot{\theta} \sin \theta) \\
& - 2fr^3\dot{\theta}^4 \csc \theta((17a-4b)\cos \theta + 3(7a+10b)fr^2\ddot{\theta} \sin \theta)) - 4fr(f^4r^9(2a\varepsilon + 2(8a+3b)\varepsilon f + r^2 \\
& + (a+b)\varepsilon \ddot{f}r^2)\dot{\theta}^9 - 12(2a+b)\varepsilon f^4r^8\dot{\theta}^8 \cot \theta - 4\varepsilon(3(20a+19b)fr^2\ddot{\theta} + b \cot \theta) + 2r\dot{\theta}(r^2 - 4(2a+b)\varepsilon \ddot{f}r^2 \\
& + 180(a+b)\varepsilon f^2r^4\ddot{\theta}^2 + 7a\varepsilon \cot^2 \theta - b\varepsilon \cot^2 \theta - 2\varepsilon f(6(5a+4b) + (28a+19b)r^2\ddot{\theta} \cot \theta) - 8a\varepsilon \csc^2 \theta) \\
& + f^3r^7\dot{\theta}^7(16a\varepsilon + 4b\varepsilon + 18(5a+2b)\varepsilon f + 5r^2 + (9a+5b)\varepsilon \ddot{f}r^2 + 5a\varepsilon \cot^2 \theta + b\varepsilon \cot^2 \theta - 4a\varepsilon \csc^2 \theta) \\
& + fr^3\dot{\theta}^3(17a\varepsilon + 7b\varepsilon + 7r^2 + 12b\varepsilon \ddot{f}r^2 - 60(a+b)\varepsilon f^2r^4\ddot{\theta}^2 + 38a\varepsilon \cot^2 \theta + 2\varepsilon f(2(82a+63b) \\
& - (47a+26b)r^2\ddot{\theta} \cot \theta) - 41a\varepsilon \csc^2 \theta - 3b\varepsilon \csc^2 \theta) + 2\varepsilon f^2r^4\dot{\theta}^4 \csc \theta((-127a-55b)\cos \theta \\
& + (29a-7b)fr^2\ddot{\theta} \sin \theta) + 2\varepsilon f^3r^6\dot{\theta}^6 \csc \theta((-49a-18b)\cos \theta + 6(2a+b)fr^2\ddot{\theta} \sin \theta) \\
& + 6\varepsilon fr^2\dot{\theta}^2 \csc \theta(-15(2a+b)\cos \theta + 2(47a+43b)fr^2\ddot{\theta} \sin \theta) + f^2r^5\dot{\theta}^5 \csc \theta((2a\varepsilon + 8b\varepsilon + 9r^2 \\
& + 24(a+b)\varepsilon \ddot{f}r^2) \sin \theta + 3\varepsilon f(2(3a+4b)r^2\ddot{\theta} \cos \theta + 3(23a+7b)\sin \theta)) - 8(-\cot \theta(r^2 - 2a\varepsilon \ddot{f}r^2 \\
& + (a+b)\varepsilon \cot^2 \theta - 2a\varepsilon \csc^2 \theta - 2b\varepsilon \csc^2 \theta) - fr(r\ddot{\theta}(-r^2 + 2(10a+9b)\varepsilon \ddot{f}r^2 + (-7a+b)\varepsilon \cot^2 \theta \\
& + 8a\varepsilon \csc^2 \theta) + r\dot{\theta}^2 \cot \theta(3a\varepsilon - b\varepsilon + 4r^2 + (5a+4b)\varepsilon \ddot{f}r^2 + 4(a+b)\varepsilon \cot^2 \theta - 9a\varepsilon \csc^2 \theta \\
& - 9b\varepsilon \csc^2 \theta) + \dot{\theta}(12(3a+2b)\varepsilon \ddot{f}r^2 + 2(2a+b)\varepsilon f^{(3)}r^3 + 1/2((9a+b)\varepsilon - 3r^2 \\
& + ((-7a+b)\varepsilon + 3r^2)\cos(2\theta))\csc^2 \theta) + 2f^5r^7\dot{\theta}^6 \csc \theta(3(2a+b)\varepsilon r\dot{\theta}^2 \cos \theta - 3(2a+b)\varepsilon \dot{\theta} \sin \theta \\
& + r^2(2a\varepsilon + b\varepsilon + r^2 + a\varepsilon \ddot{f}r^2)\dot{\theta}^3 \sin \theta - 3(2a+b)\varepsilon r\ddot{\theta} \sin \theta) - f^2r(r^2(-2a\varepsilon - 6b\varepsilon - 11r^2 + 2(24a+13b)\varepsilon \ddot{f}r^2 \\
& + 2(5a+2b)\varepsilon f^{(3)}r^3)\dot{\theta}^3 + r\dot{\theta}^2(r^2(4a\varepsilon - 8b\varepsilon - 3r^2 + 6(a+b)\varepsilon \ddot{f}r^2)\dot{\theta} + 3(15a+7b)\varepsilon \cot \theta) \\
& + 6\varepsilon \dot{\theta}(a+b + (15a+11b)r^2\ddot{\theta} \cot \theta) + r^3\dot{\theta}^4 \cot \theta(4(5a+2b)\varepsilon \ddot{f}r^2 - 3/2(5a\varepsilon + 9b\varepsilon - 2r^2 \\
& + (a\varepsilon - 3b\varepsilon + 2r^2)\cos(2\theta))\csc^2 \theta) + 6(a+b)\varepsilon r\ddot{\theta} \csc \theta(2r^2\ddot{\theta} \cos \theta + 9 \sin \theta) \\
& - 1/2f^4r^5\dot{\theta}^2(240(a+b)\varepsilon r^2\ddot{\theta}^2 + 240(a+b)\varepsilon r^3\ddot{\theta}^3 - 4\varepsilon \dot{\theta}^3(-9b + (20a+17b)r^2\ddot{\theta} \cot \theta) \\
& + 2r^2\dot{\theta}^5(-26a\varepsilon - 16b\varepsilon - 9r^2 + 3(-a+b)\varepsilon \ddot{f}r^2 + 2a\varepsilon f^{(3)}r^3 - 2a\varepsilon \cot^2 \theta - 8b\varepsilon \cot^2 \theta + 6b\varepsilon \csc^2 \theta) \\
& - 2r\dot{\theta}^4(2(22a+13b)\varepsilon \cot \theta + r^2\ddot{\theta}(8a\varepsilon + 8b\varepsilon + r^2 + 4a\varepsilon \ddot{f}r^2 - 2(a-b)\varepsilon \cot^2 \theta + 4a\varepsilon \csc^2 \theta)) \\
& - 12\varepsilon r\dot{\theta}^2\dot{\theta} \csc \theta(8(a+b)r^2\ddot{\theta} \cos \theta + (-8a-11b)\sin \theta) + r^3\dot{\theta}^6 \cot \theta \csc^2 \theta(-2a\varepsilon - 6b\varepsilon + r^2 \\
& - (2a\varepsilon - 2b\varepsilon + r^2)\cos(2\theta) + 8a\varepsilon \ddot{f}r^2 \sin^2 \theta)) - 1/2f^3r^3(-600(a+b)\varepsilon r^2\ddot{\theta}^2 - 40(a+b)\varepsilon r^3\dot{\theta}^3 \\
& + 2\varepsilon \dot{\theta}^3(-3(37a+29b) + 2(25a+16b)r^2\ddot{\theta} \cot \theta) - 2r\dot{\theta}^4((-13a-b)\varepsilon \cot \theta + r^2\dot{\theta}(16a\varepsilon + 16b\varepsilon + 3r^2 \\
& + 6(3a+2b)\varepsilon \ddot{f}r^2 + 3(a+b)\varepsilon \cot^2 \theta)) + 2r^2\dot{\theta}^5(-35a\varepsilon - 23b\varepsilon - 15r^2 + (11a+5b)\varepsilon \ddot{f}r^2 + 2(4a+b)\varepsilon f^{(3)}r^3 \\
& - 6a\varepsilon \cot^2 \theta - 12b\varepsilon \cot^2 \theta + 3a\varepsilon \csc^2 \theta + 9b\varepsilon \csc^2 \theta) - 2\varepsilon r\dot{\theta}^2\ddot{\theta} \csc \theta(36(a+b)r^2\ddot{\theta} \cos \theta \\
& + (295a+271b)\sin \theta) - r^3\dot{\theta}^6 \cot \theta \csc^2 \theta(9a\varepsilon + 21b\varepsilon - 4r^2 + (5a\varepsilon - 7b\varepsilon + 4r^2)\cos(2\theta) \\
& - 2(17a+4b)\varepsilon \ddot{f}r^2 \sin^2 \theta))],
\end{aligned}
\tag{A.1}$$

$$\begin{aligned}
A_4 = & \frac{1}{188697600A_1^5(a+b)\varepsilon r^6} [32A_1^3r^3(-15263640A_2^3(a+b)\varepsilon r^3 + 1260A_1^2\varepsilon r(-491aA_2 - 608A_2b \\
& + 2573aA_3r + 2540A_3br) - 5040A_1A_2\varepsilon r^2(A_2(497a + 503b) - 4606A_3(a+b)r) \\
& + 420A_1^5r(-65a\varepsilon - 38b\varepsilon + 6r^2) + A_1^9r^3(-6a\varepsilon - 34b\varepsilon + 7r^2) + 14A_1^7r^2(46a\varepsilon + 40b\varepsilon + 15r^2) \\
& + 21A_1^6A_2r^3(222a\varepsilon - 38b\varepsilon + 65r^2) - 630A_1^3(2(71a + 176b)\varepsilon + A_2^2r^3(27a\varepsilon - 41b\varepsilon + 17r^2)) \\
& + 210A_1^4r^2(A_3r(983a\varepsilon + 1067b\varepsilon - 21r^2) + A_2(490a\varepsilon + 160b\varepsilon + 93r^2)) \\
& + (1/(f^3))7(-33177600(a+b)\varepsilon + A_1r(90A_1\varepsilon\dot{f}r(-512(616a + 601b) - 128A_1^2(611a + 581b)\dot{f}r^2 \\
& - 32A_1^4(67a + 119b)\dot{f}^2r^4 + 40A_1^6(3a+b)\dot{f}^3r^6 - A_1^8(a+b)\dot{f}^4r^8) + 15f(-1536(4A_1(646a + 631b)\varepsilon \\
& + 7383A_2(a+b)\varepsilon r + A_1^3r(19(a+b)\varepsilon + r^2)) + A_1^2r^2(768A_1(267a + 248b)\varepsilon\ddot{f}r \\
& + 6A_1^6(a+b)\varepsilon\dot{f}^4r^6(4A_1 + 15A_2r) + A_1^4\varepsilon\dot{f}^3r^4(-48A_1(47a + 17b) + 8(5a(A_1^3 - 96A_2) \\
& + (A_1^3 - 150A_2)b)r + 21A_1^3(a+b)\ddot{f}r^3) + 16\dot{f}(120A_1^3r^3 + 3A_1^3(491a + 685b)\varepsilon\ddot{f}r^3 \\
& - 8\varepsilon(9138aA_1 + 8802A_1b + 253aA_1^3r + 28668aA_2r + 163A_1^3br + 28038A_2br)) \\
& + 8A_1^2\dot{f}^2r^2(240A_1(9a - 5b)\varepsilon - 48A_2(137a + 148b)\varepsilon r - 3A_1^3(83a + 29b)\varepsilon\ddot{f}r^3 \\
& - 4A_1^3r(53a\varepsilon + 55b\varepsilon + 9r^2)) + 4A_1^5f^3r^4(90A_1^2\varepsilon\dot{f}^2r^2(A_1^2(41a + 15b) + 15A_1A_2(25a + 9b)r \\
& + 5(18A_2^2 + 5A_1A_3)(3a + b)r^2) + 3\dot{f}(16A_1^6(2a + b)\varepsilon r^2 - 24480A_2^2(2a + b)\varepsilon r^2 \\
& + 720A_1\varepsilon r(87aA_2 + 36A_2b - 14A_3(2a + b)r) + 60A_1^4r(5a\varepsilon + 2b\varepsilon + 9r^2) + 30A_1^3r^2(25A_3r(2a\varepsilon + r^2) \\
& + 4A_2(97a\varepsilon + 41b\varepsilon + 30r^2)) + 180A_1^2(-8(2a + b)\varepsilon + 15A_2^2(2a\varepsilon r^3 + r^5)) + 15A_1^2\varepsilon r^3(2\dot{f}(3A_1^2(20a + 7b) \\
& + 30A_1A_2(7a + 3b)r + 5(18A_2^2 + 5A_1A_3)(a + b)r^2) + A_1r(A_1(a + b)f^{(4)}r + 2f^{(3)}(A_1(11a + 5b) \\
& + 15A_2(a + b)r))) + r(90A_1^3\varepsilon\dot{f}^2r^3(A_1(9a + 5b) + 15A_2(a + b)r) + \dot{f}(135A_1^4(a + b)\varepsilon f^{(3)}r^4 \\
& + 270A_1^3r^3(2A_1 + 5A_2r) + 4\varepsilon(1080A_1^2(3a + b) + 15A_1(52aA_1^3 - 1788aA_2 + 15A_1^3b - 828A_2b)r \\
& + a(8A_1^6 + 2235A_1^3A_2 - 12240A_2^2 - 5040A_1A_3)r^2)) + 15A_1r(-192aA_1\varepsilon f^{(4)}r \\
& + f^{(3)}(-48A_1(19a + 6b)\varepsilon - 2208aA_2\varepsilon r + A_1^3(38a\varepsilon r + 3r^3)))) - A_1f^2r(384(270A_1^2(249a + 239b)\varepsilon \\
& + 619200A_2^2(a + b)\varepsilon r^2 + 30A_1\varepsilon r(15A_2(697a + 683b) - 6682A_3(a + b)r) + 30A_1^4r(77a\varepsilon + 55b\varepsilon - 3r^2) \\
& + 15A_1^3A_2r^2(247a\varepsilon + 203b\varepsilon + 7r^2) - A_1^6r^2(23a\varepsilon + 3b\varepsilon + 10r^2)) + A_1^2r^2(90A_1^4(a + b)\varepsilon\dot{f}^3r^4(6A_1^2 + 90A_2^2r^2 \\
& + 5A_1r(12A_2 + 5A_3r)) + A_1^2\varepsilon\dot{f}^2r^2(8(-360A_1^2(8a + 3b) + 30A_1(5aA_1^3 - 939aA_2 + A_1^3b - 339A_2b)r \\
& + (A_1^6 + 195A_1^3A_2 - 1530A_2^2 - 630A_1A_3)(5a + b)r^2) + 135A_1^3(a + b)r^3(A_1f^{(3)}r + \ddot{f}(8A_1 + 30A_2r))) \\
& + 240A_1r(15A_1(49a + 39b)\varepsilon f^{(3)}r + \dot{f}(24A_1(52a - 15b)\varepsilon - 6A_2(457a + 587b)\varepsilon r - 3A_1^3(19a + 7b)\varepsilon\ddot{f}r^3 \\
& - 2A_1^3r(76a\varepsilon + 50b\varepsilon + 9r^2))) + 6\dot{f}(-720A_1^3r^3(2A_1 + 9A_2r) - 16\varepsilon(60A_1^2(105a - 4b) + 20A_1(25aA_1^3 \\
& - 330aA_2 + 6A_1^3b - 261A_2b)r + (a(7A_1^6 + 1080A_1^3A_2 - 30060A_2^2 + 38265A_1A_3) + 3(3A_1^6 + 190A_1^3A_2 \\
& - 9780A_2^2 + 13085A_1A_3)b)r^2) + 5A_1^3\varepsilon r^3(-24A_1(19a + 7b)f^{(3)}r + \dot{f}(-48A_1(51a + 19b) \\
& + 8(5aA_1^3 - 588aA_2 + A_1^3b - 204A_2b)r + 9A_1^3(a + b)\ddot{f}r^3)))) - 24A_1^5f^4r^3(4(2a + b)\varepsilon(-180A_1^2 \\
& + 1620A_1A_2r + (2A_1^6 + 165A_1^3A_2 - 3060A_2^2 - 1260A_1A_3)r^2 - 75A_1^2(18A_2^2 + 5A_1A_3)r^3) \\
& - 60A_1^2r^3(3A_1^2 + 90A_2^2r^2 + 5A_1r(9A_2 + 5A_3r)) - 15A_1^2\varepsilon r^2(2(8a + 3b)\dot{f}(A_1^2 + 90A_2^2r^2 \\
& + 5A_1r(6A_2 + 5A_3r)) + r(2\dot{f}(2A_1^2(11a + 3b) + 15A_1A_2(14a + 3b)r \\
& + 10a(18A_2^2 + 5A_1A_3)r^2) + A_1r(2aA_1f^{(4)}r + f^{(3)}(3A_1b + 20a(A_1 + 3A_2r)))))))] |_{r_1} ,
\end{aligned}$$

$$\begin{aligned}
A_2 = & \frac{1}{26880A_1(a+b)\varepsilon fr^2} [(-14592(a+b)\varepsilon + A_1^2r(3\varepsilon\dot{f}r(-16(29a + 35b) + 8A_1^2(5a + b)\dot{f}r^2 \\
& - A_1^4(a+b)\dot{f}^2r^4)24A_1^2f^2r(2A_1^2r^3 + 2(2a + b)\varepsilon(12 + A_1^2r) + A_1^2\varepsilon r^2((8a + 3b)\dot{f} + 2a\ddot{f}r)) \\
& + 4f(-8(6(31a + 28b)\varepsilon + A_1^2r(19a\varepsilon + 7b\varepsilon + 3r^2)) + 3A_1^2r^2(\varepsilon\ddot{f}r(-32a + A_1^2(a + b)\dot{f}r^2) \\
& + \dot{f}(-48(2a + b)\varepsilon + A_1^2(3a + b)\varepsilon\dot{f}r^2 + A_1^2r(2a\varepsilon + r^2)))))] |_{r_1} ,
\end{aligned}$$

$$\begin{aligned}
A_3 = & \frac{1}{1140480A_1^3(a+b)\varepsilon r^4} [(15\varepsilon(56576(a+b) + 384A_1^2(74a+69b)\dot{f}r^2 + 32A_1^4(37a+57b)\dot{f}^2r^4 \\
& - 8A_1^6(10a+3b)\dot{f}^3r^6 + A_1^8(a+b)\dot{f}^4r^8))/f^2 + 120A_1^5fr^3(6A_1^2r^3(A_1+5A_2r) \\
& - 2(2a+b)\varepsilon(12A_1+A_1^3r-84A_2r-15A_1^2A_2r^2) + A_1^2\varepsilon r^2((8a+3b)\dot{f}(2A_1+15A_2r) \\
& + r(2aA_1f^{(3)}r + \ddot{f}(14aA_1+3A_1b+30aA_2r)))) + (1/f)5A_1r(64(30A_1(101a+95b)\varepsilon \\
& + 9372A_2(a+b)\varepsilon r + A_1^3r(79a\varepsilon+67b\varepsilon-9r^2)) + A_1^2r^2(-144A_1(35a+33b)\varepsilon\dot{f}r \\
& - 3A_1^4(a+b)\varepsilon\dot{f}^3r^4(4A_1+15A_2r) + A_1^2\varepsilon\dot{f}^2r^2(24A_1(37a+13b) - 4(A_1^3-42A_2)(5a+b)r \\
& - 9A_1^3(a+b)\ddot{f}r^3) + 16\dot{f}(12A_1(-30a+13b)\varepsilon + 3A_2(517a+523b)\varepsilon r + 12A_1^3(3a+b)\varepsilon\dot{f}r^3 \\
& + A_1^3r(40a\varepsilon+34b\varepsilon+9r^2)))) + 4A_1^2r^2(4(180A_1^2(25a+32b)\varepsilon + 180A_1A_2(173a+172b)\varepsilon r \\
& + 123480A_2^2(a+b)\varepsilon r^2 + 30A_1^3A_2r^2(37a\varepsilon+65b\varepsilon-7r^2) + 30A_1^4r(30a\varepsilon+16b\varepsilon+3r^2) \\
& + A_1^6r^2(6a\varepsilon-14b\varepsilon+5r^2)) + 5A_1^3r^2(3A_1^2\varepsilon\dot{f}^2r^2(A_1(25a+9b) + 15A_2(3a+b)r) \\
& + 3\dot{f}(8A_1(29a+12b)\varepsilon - 336A_2(2a+b)\varepsilon r + 15A_1^2A_2r^2(2a\varepsilon+r^2) + 4A_1^3r(7a\varepsilon+3b\varepsilon+2r^2) \\
& + A_1^2\varepsilon r^3(A_1(a+b)f^{(3)}r + \ddot{f}(2A_1(7a+3b) + 15A_2(a+b)r))) + r(-144aA_1\varepsilon f^{(3)}r \\
& + \ddot{f}(-72A_1(7a+3b)\varepsilon - 672aA_2\varepsilon r + 3A_1^3(a+b)\varepsilon\dot{f}r^3 + A_1^3(22a\varepsilon r + 3r^3)))))] |_{r_1} .
\end{aligned} \tag{A.4}$$

-
- [1] A. Flachi and T. Tanaka, Phys. Rev. Lett. **95**, 161302 (2005).
- [2] V. P. Frolov, Phys. Rev. D **74**, 044006 (2006).
- [3] D. Mateos, R. C. Myers and R. M. Thomson, Phys. Rev. Lett. **97**, 091601 (2006).
- [4] F. Mena, J. Natario and P. Tod, *Formation of Higher Dimensional Topological Black Holes*, Annales Henri Poincaré **10** (2010), 1359-1376;
- [5] B. Kol, J. High Energy Phys. **10** (2005) 049.
- [6] B. Kol, Phys. Rep. **422**, 119 (2006).
- [7] D. Mateos, R. C. Myers and R. M. Thomson, J. High Energy Phys. **05** (2007) 067.
- [8] J. Maldacena, Adv. Theor. Math. Phys. **2**, 231-252 (1998).
- [9] P. A. M. Dirac, Proc. R. Soc. A. **268**, 57 (1962).
- [10] J. Nambu, Copenhagen Summer Symposium (1970), unpublished.
- [11] T. Goto, Prog. Theor. Phys. **46**, 1560 (1971).
- [12] V. P. Frolov and D. Gorbonos, Phys. Rev. D **79**, 024006 (2009).
- [13] V. G. Czinner and A. Flachi, Phys. Rev. D **80**, 104017 (2009).
- [14] V. G. Czinner, Phys. Rev. D **82**, 024035 (2010).
- [15] F. R. Thangerlini, Nuovo Cimento **77**, 636 (1963).
- [16] B. Carter and R. Gregory, Phys. Rev. D **51**, 5839 (1995).
- [17] E. T. Whittaker, *Analytical Dynamics*, Cambridge University Press, London, 1937, 4th ed., p. 266.
- [18] A. Flachi, O. Pujolás, M. Sasaki and T. Tanaka, Phys. Rev. D **73**, 125017 (2006).
- [19] A. Flachi and T. Tanaka, Phys. Rev. D **76**, 025007 (2007).
- [20] C. M. Bender and S. A. Orszag, *Advanced Mathematical Methods for Scientists and Engineers*, McGraw-Hill, Inc. New York, 1978, p. 63.
- [21] K. Hioki, U. Miyamoto and M. Nozawa, Phys. Rev. D **80**, 084011 (2009).